Journal of Hazardous Materials 192 (2011) 651–657

Contents lists available at ScienceDirect

Journal of Hazardous Materials

journal homepage: www.elsevier.com/locate/jhazmat

Microemulsion-mediated solvothermal synthesis and photocatalytic properties of crystalline titania with controllable phases of anatase and rutile

Xiaojun Shen, Jinlong Zhang*, Baozhu Tian

Key Laboratory for Advanced Materials and Institute of Fine Chemicals, East China University of Science and Technology, 130 Meilong Road, Shanghai 200237, PR China

ARTICLE INFO

Article history:
Received 27 January 2011
Received in revised form 30 April 2011
Accepted 21 May 2011
Available online 1 June 2011

Keywords:
Titanium oxide
Phase control
Nanostructures
Microemulsion
Solvothermal synthesis

ABSTRACT

Titanium oxide with different ratios of anatase to rutile has been prepared by the microemulsion-mediated solvothermal method. The resulting samples were investigated by X-ray diffraction, Raman spectroscopy, scanning electron microscopy, UV–vis diffuse reflectance spectra, transmission electron microscopy and Brunauer–Emmett–Teller analysis. The contents of anatase and rutile in the TiO_2 particles have been successfully controlled by simply adjusting the amount of urea in the aqueous phase of the microemulsion. Both the degradation of Rhodamine B in aqueous solutions and mineralization of TOC revealed that the catalyst containing 47.6% anatase have presented the highest photocatalytic activity. A proposed mechanism is discussed to interpret the evolution of the phases based on the effect of different amount of urea.

1. Introduction

Titanium dioxide has attracted much attention because of its specific properties: photocatalytic activity, photovoltaic effects, long-term stability, nontoxicity, and low cost [1–3]. The application for TiO_2 strongly depends upon the crystal structure, morphology, and size of the particles. TiO_2 exists mainly in three crystalline forms: anatase, rutile and brookite. Each crystalline form has different physiochemical properties, such as density, refractive index, and photochemical reactivity. With a high density and refractive index, rutile has been widely employed in fields of pigments, optical devices, etc. Anatase generally shows higher photocatalytic activity in the photodegradation of most pollutants in water and air, while the photocatalytic performance of rutile is still indistinct [4–6]. Brookite is the least studied because of the difficulties in synthesizing the pure form, though it was reported to show remarkable photocatalytic activity [7]. However, much experimental evidence indicates that mixed phases, such as anatase/rutile [8,9], brookite/rutile [10,11], and brookite/anatase [12,13], exhibit evident synergistic effects on enhancing the photocatalytic activity. Therefore, it is of great important to develop an effective method to synthesize mixed-phase TiO_2 with tunable ratios of two phases.

In general, phase composition and particle size of TiO_2 prepared by solution-phase methods are depended upon the temperature, pH, type and concentration of reactants. The effects of pH on TiO_2 phase structure have been studied by several groups [14–16], and it is commonly assumed that low pH favors the formation of rutile phase while high pH favors anatase, but these studies did not show us a precise manner of controlling the TiO_2 crystalline phase with stepwise adjustment of the proportion of anatase or rutile.

Water-in-oil (W/O) microemulsions with nanosized aqueous cores have been extensively used as the reaction media for preparation of nanomaterials [17,18]. In microemulsions, the reactants are well dispersed in the extremely small reactor and a uniform nucleation occurs. Wu et al. [17] and Yan et al. [9] have successfully synthesized rutile and anatase with the microemulsion-mediated hydrothermal method. However, tetrabutyl titanate has been used as the precursor in these cases, which will be hydrolyzed unavoidably in water, even in moist air. Herein, based on these studies, we report a microemulsion-mediated solvothermal method to synthesize mixed-phase TiO_2 nanocrystals with a tunable anatase/rutile ratio and to investigate the influence of the pH value on the formation of anatase and rutile. Titanium trichloride is chosen as the titanium source, which can be easily manipulated and urea as the "in situ pH adjusting reagent". The ratio of anatase to rutile in mixed-phase TiO_2 nanocrystals is able to be easily tuned by simply changing the additional amount of urea in aqueous phase of microemulsion. To confirm the effect of mixed anatase and rutile

* Corresponding author. Tel.: +86 21 64252062; fax: +86 21 64252062.
E-mail address: jlzhang@ecust.edu.cn (J. Zhang).

0304-3894/$ – see front matter © 2011 Elsevier B.V. All rights reserved.
doi:10.1016/j.jhazmat.2011.05.066

phases on the photocatalytic activity, the performance of prepared TiO_2 with different ratios of anatase to rutile was achieved for the photodegradation of Rhodamine B.

2. Experimental

2.1. Synthesis of mixed-phase TiO_2 catalysts

The synthetic procedure of reverse microemulsion system was as follows: First, 10 mL of Triton X-100 (surfactant), 6 mL of *n*-hexanol (cosurfactant), and 16 mL of cyclohexane (oil phase) were mixed under magnetic stirring. Second, 2.0 mL of 15% $TiCl_3$ solution and specific amount of urea were dissolved in 2.0 mL of water (series I) or 10 M hydrochloric acid solution (series II), making up the aqueous phase. Then, the aqueous phase was added dropwise to the oil phase under stirring at room temperature for 4 h, forming the clear microemulsion. The microemulsion was heated at 180 °C for 12 h in the autoclave. The precipitate was collected by centrifugation and washed repeatedly with ethanol and water, and then dried under vacuum at 60 °C for 6 h. The samples are labeled as SN-T, where N is a series number and T is the addition amount of urea. The SI-0.30 represents the sample that obtained in series I, in which 0.30 g urea was dissolved in water. The SII-0.90 refers to 0.90 g urea dissolved in 10 M hydrochloric acid solution.

2.2. Characterization

The synthesized mixed-phase TiO_2 samples were characterized by X-ray diffraction (XRD), scanning electron microscopy (SEM), Raman spectroscopy, UV–vis diffuse reflectance spectra (DRS), transmission electron microscopy (TEM) and Brunauer–Emmett–Teller (BET) analysis. The XRD patterns of as-prepared products, recorded on a Rigaku D/max 2550 VB/PC diffractometer using Cu Kα radiation ($\lambda = 0.15405$ nm, voltage 40 kV, current 100 mA) and a secondary graphite monochromator in the 2θ range from 10° to 80° (2θ steps 0.02°, count time of 2 s per step), were used to identify the crystal structures and crystallite sizes. The morphology of titania was observed by using scanning electron microscopy (JSM-6360LV) and transmission electron microscopy (JEOL JEM-2011). The TEM samples were prepared by dropping an alcohol suspension of powders on a carbon-coated copper grid, operated at an accelerating voltage of 120 and 200 kV. UV–vis spectra were obtained for dry-pressed disk samples using a Shimadzu UV-2450 PC instrument. $BaSO_4$ powder was used as a reference, and the spectra were recorded in the range 200–800 nm. The BET specific surface area measurements of the samples were determined by the N_2 adsorption–desorption method at 77 K (Micromeritics, ASAP 2010), after being degassed at 453 K for 10 h.

2.3. Photocatalytic activities

The photocatalytic activities of the products were evaluated by degrading Rhodamine B in an aqueous solution. A 300-W high-pressure Hg lamp was used as the light source, which had been positioned inside a quartz cylindrical vessel and cooled by a circulating water jacket. 0.06 g of TiO_2 was suspended in 60 mL of aqueous Rhodamine B (20 mg L^{-1}). Before the photocatalytic experiment, the suspension was continuously stirred for 30 min in dark in order to establish the adsorption–desorption equilibrium among TiO_2, Rhodamine B, and dissolved oxygen. The concentration of Rhodamine B was analyzed by measuring the maximum absorbance on a UV–vis spectrometer. Reference experiment was performed by using Degussa P25 titanium dioxide as photocatalyst. The TiO_2 powder was separated from the solution by centrifugation, and the clear upper solution was analyzed for the total organic carbon (TOC). TOC was determined using a Shimadzu TOC-VE analyzer.

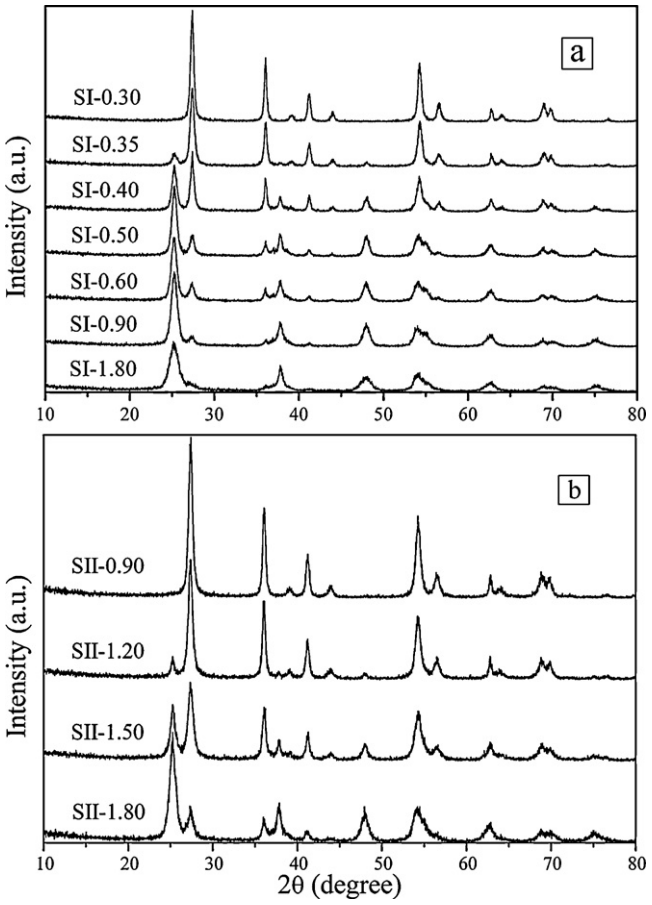

Fig. 1. XRD patterns of TiO_2 synthesized with different reaction series: (a) series I, (b) series II.

3. Results and discussion

3.1. Phase structure, composition and morphology of TiO_2 products

3.1.1. Analysis of XRD and BET

As shown in Fig. 1, the XRD patterns illustrate the crystalline phase evolution of TiO_2 synthesized with different addition amount of urea. In series I, the samples are pure rutile when the amount of urea is ≤0.30 g (only the pattern of SI-0.30 is presented). The anatase phase appears when the addition amount of urea is ≥0.35 g, and the content of anatase increases in the order of SI-0.35, SI-0.40, SI-0.50, SI-0.60, SI-0.90, and SI-1.80. When the addition of urea is adjusted to 1.80 g, the obtained TiO_2 powder is almost pure anatase phase. That is to say, the contents of anatase and rutile in samples can be successfully controlled by simply adjusting the addition amount of urea. Comparing with series I, the composition of aqueous phase was changed in series II, in which $TiCl_3$ and urea were dissolved in 10 M HCl solution instead of water. The crystalline phase evolution of TiO_2 in series II (Fig. 1b) is similar to that of series I, but detailed adding amount of urea is different. In series II, the samples are pure rutile when the applied urea is ≤0.90 g; anatase appears with further increasing the addition amount of urea in the aqueous phase. The required amount of urea to control the phase increases obviously in series II. For example, the main phase of product is anatase when the amount of urea is 0.90 g in series I. In contrast, the product is still pure rutile in series II.

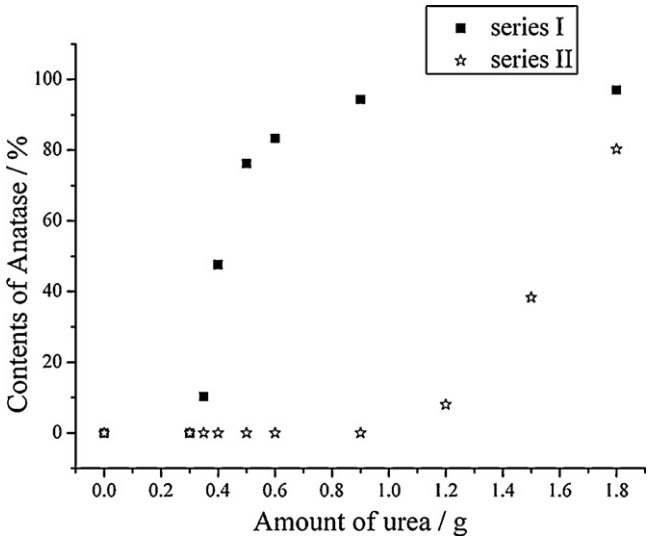

Fig. 2. Relationship between the contents of anatase and the applied amount of urea in the aqueous phase in reaction series I and II.

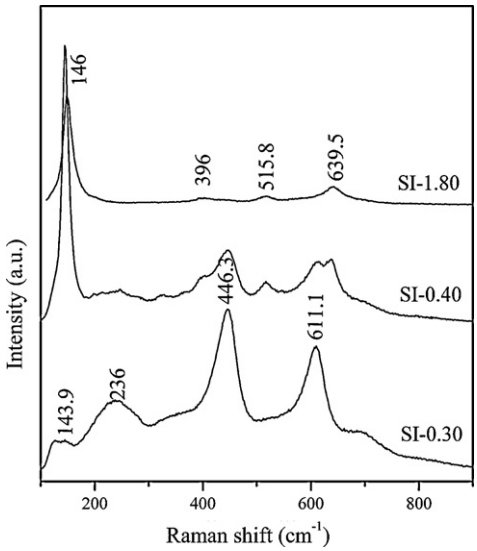

Fig. 3. Raman spectra of the three samples shown in Fig. 1a: SI-0.30, SI-0.40, and SI-1.80.

The average crystalline sizes of anatase and rutile in samples are calculated by applying the Debye–Scherrer formula on the anatase (1 0 1) and rutile (1 1 0) diffraction peaks, and the relative phase contents of the samples are estimated from the respective XRD peak intensities using the following equation [19]

$$W_A = \frac{K_A I_A}{(K_A I_A + I_R)};$$

$$W_R = \frac{I_R}{(K_A I_A + I_R)};$$

$$K_A = 0.886$$

where W_A and W_R are the fraction of anatase and rutile, and I_A and I_R are the peak areas of the anatase (1 0 1) and rutile (1 1 0) diffraction peaks, respectively. The results of the average crystalline sizes and phase composition are calculated and shown in Table 1.

To study the relationship between the contents of anatase and the amount of urea intuitively, an illustration was carried out to show the trend of phase composition in two series (Fig. 2). Interestingly, it was found that two curves, presenting the relationship between the contents of anatase and the amount of urea in series I and II, would make up of a closed curve. It is reasonably believed that the phase composition of as-prepared products with changing the acidity of the aqueous phase would locate within the area of the closed curve. The acidity of aqueous phase could be controlled by varying the concentration of additional hydrochloric acid solution, which can change from 0 M (series I) to 10 M (series II). It implied that we could control the phases of the products located in the region enclosed by such a curve through changing the acidity of aqueous phase and the amount of urea.

The surface areas (S_{BET}) of the samples are estimated by the BET method (shown in Table 1). It is found that S_{BET} values show the uptrend with further increasing the anatase content both in series I and II. The average crystalline size of anatase decreases with increasing the amount of urea, resulting in the increase of S_{BET}.

3.1.2. Analysis of raman spectra

The phase structures of TiO_2 powders were further characterized by Raman spectroscopy in Fig. 3. Anatase exhibits characteristic scatterings at 144 (E_g), 397 (B_{1g}), 517 (A_{1g}) and 639 cm^{-1} (E_g) [20], while rutile gives typical scatterings at 143 (B_{1g}), 235 (two-phonon scattering), 447 (E_g), and 612 cm^{-1} (A_{1g}) [21]. Fig. 3 shows Raman spectra of the three powders of SI-0.30, SI-0.40 and SI-1.80. Both the position and the relative intensity of the observed Raman bands are in good accordance with the literature, from which phase composition of the powders was confirmed. It is indicated that the phase of SI-0.30 is rutile and that of SI-1.80 is anatase, while SI-0.40 consists of both anatase and rutile. The results are in agreement with the XRD data.

3.1.3. Analysis of SEM and TEM

It can be found that the content of anatase phase increases with the amount of urea both in series I and II. The average crystalline size of anatase decreases with increasing the amount of urea, which may be induced by the different acidity of solution in system, such as the final size decreases with increasing pH [15]. Besides the changes of crystalline phases, the morphologies of particles also vary with the preparation conditions. The typical SEM and TEM

Table 1
Synthetic conditions, phase contents, crystalline sizes and BET surface areas of TiO_2 particles.

Sample	Amount of urea (g)	Contents of rutile (%)	Contents of anatase (%)	Crystalline size of rutile (nm)	Crystalline size of anatase (nm)	S_{BET} (m^2/g)
SI-0.30	0.30	100	0	22.8		34
SI-0.35	0.35	89.3	10.7	18.6	16.9	62
SI-0.40	0.40	52.4	47.6	20.6	16.0	62
SI-0.50	0.50	23.8	76.2	16.4	15.0	67
SI-0.60	0.60	16.7	83.3	19.6	14.1	77
SI-0.90	0.90	5.7	94.3	17.2	12.5	98
SI-1.80	1.80	3.0	97.0	10.7	10.1	112
SII-0.90	0.90	100	0	18.8		49
SII-1.20	1.20	92.0	8.0	18.1	19.8	60
SII-1.50	1.50	61.7	38.3	14.8	16.6	72
SII-1.80	1.80	19.2	80.8	14.2	13.1	89

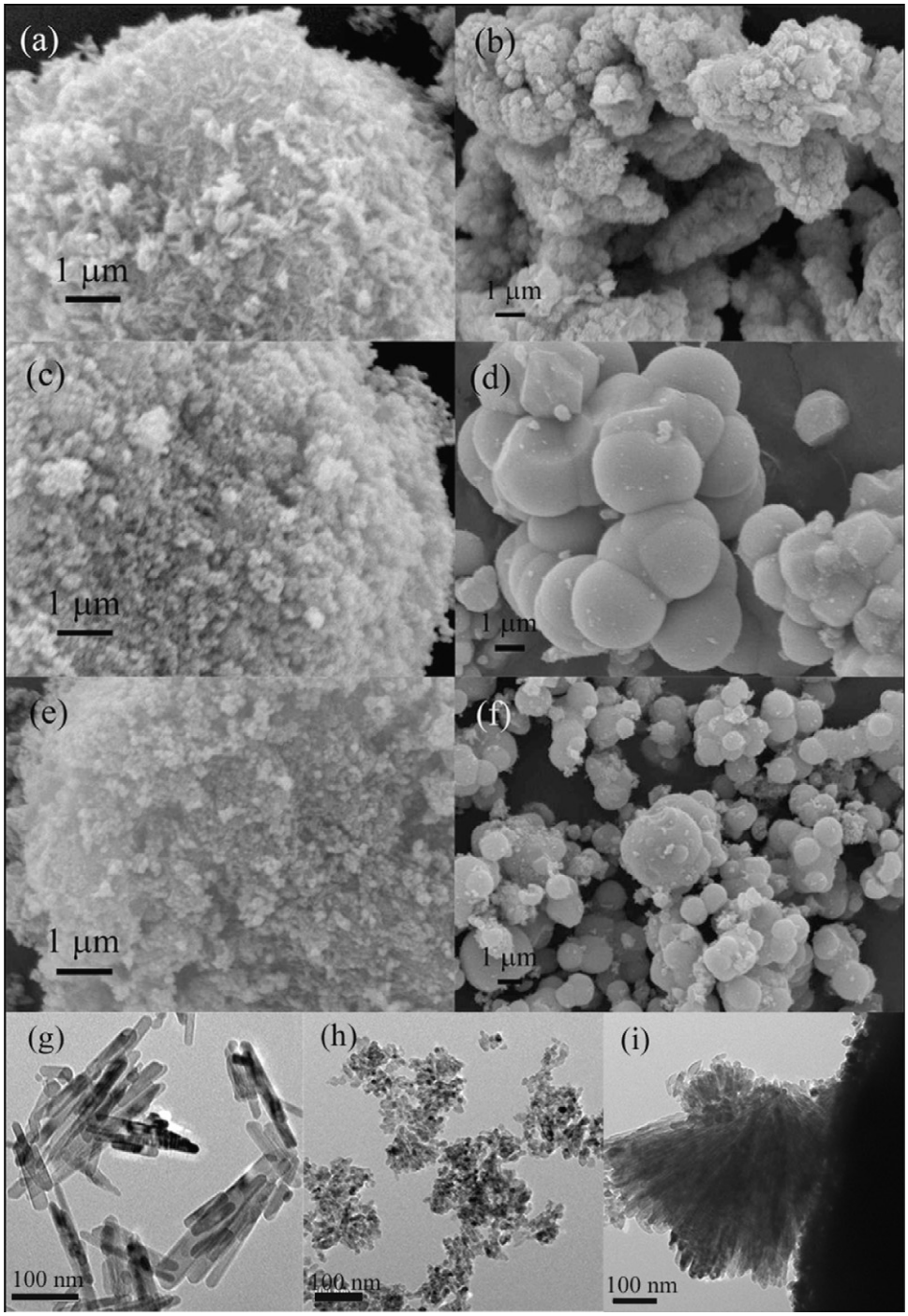

Fig. 4. SEM (a)–(f) and TEM (g)–(i) images of different samples: (a) and (g) SI-0.30, (b) SII-0.30, (c) and (h) SI-0.90, (d) and (i) SII-0.90, (e) SI-1.80, (f) SII-1.80.

images of two series are shown in Fig. 4. The obtained products in series I are aggregated by small particles and the surfaces are rough; the morphologies of aggregates in series I do not change much with increasing the amount of urea (Fig. 4a, c and e). The only difference among them is that SI-0.30 is aggregated by small rodlike particles (Fig. 4a); however, the others are aggregated by small quasi-spherical particles (Fig. 4c and e). It is confirmed by the TEM images of SI-0.30 and SI-0.90. Rutile particles (SI-0.30) show elongated rodlike shape with 20–25 nm in the diameter range and lengths in the range of 100–150 nm (Fig. 4g), whereas SI-0.90 (almost anatase phase) contains about 10–15 nm quasi-spherical nanoparticles (Fig. 4h). In contrast to series I, the morphologies of the fabricated products in series II change much more with increasing the amount of urea. The crystalline form of SII-0.30 is rutile, and the morphology is loose and irregular, composed of small particles (Fig. 4b). The phase of SII-0.90 is also rutile; however, it is composed of interconnected microspheres (Fig. 4d). The TEM image (Fig. 4i) reveals that these microspheres are composed of radially aligned nanorods. It is indicted that the growth of particles has been hindered, due to the diffusion limitation with spatial constraints. Fig. 4f shows that the diameter of the microparticles slightly decreased with increasing the amount of urea to 1.80 g and it was composed of many individual quasi-spherical particles. Comparing series I and II, we could find that the acidity of the initial aqueous phase has

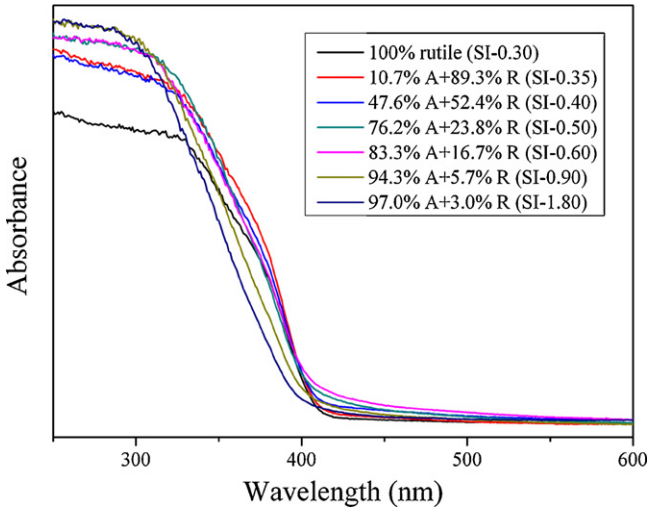

Fig. 5. UV–vis diffuse reflectance spectra of samples in Series-I: SI-0.30, SI-0.35, SI-0.40, SI-0.50, SI-0.60, SI-0.90, and SI-1.80.

an important effect on the morphologies of the final products. It is indicated that the higher acidity and concentration of Cl^- play the key role in the formation of particles. In a highly acidic solution, the high concentration of H^+ suppresses the hydrolysis of Ti^{3+} and results in a low reaction rate. However, urea, as an in situ pH adjusting reagent, is used to promote the hydrolysis. The Cl^- ions in the system can selectively adsorb on the (1 1 0) plane and influence the growth of TiO_2. Consequently, the change of morphologies may be caused by the synergistic effect of acidity and concentration of Cl^- in system. The formation of TiO_2 is retarded by changing the coordination structure of the growing unit, and Cl^- may be adsorbed on the surfaces of TiO_2 to influence the morphologies [22–24].

3.1.4. Analysis of UV–vis diffuse reflectance spectra

UV–vis diffuse reflectance spectra of the samples in series-I are presented in Fig. 5. The UV–vis DRS reflects the band gap between the valence band and the conduction band of TiO_2. As shown in Fig. 5, with the increasing proportion of rutile in the mixed-phase samples, the absorption edge gradually shifts from 395 nm to 415 nm, implying that the band gap values of TiO_2 obtained were decreased. The band gap (E_g) can be estimated by the Kubella–Munk function [25]

$$\alpha(h\nu) = C_1(h\nu - E_g)^2$$

$$h\nu = \frac{1240}{\lambda}$$

where α is the optical absorption coefficient, $h\nu$ is the photon energy, C_1 is the absorption constant for an indirect transition, and λ is the wavelength (nm). The pure rutile (SI-0.30) has a band gap energy of 2.98 eV, with the absorption started with 415 nm. The absorption of SI-1.80 starts with 395 nm, exhibiting a band gap energy value of 3.14 eV. The result is consistent with the fact that the conduction band edge of rutile is about 0.2 eV more positive than that of anatase [26]. For other samples, the band gap values show a slight increase in the order of SI-0.40, SI-0.50, SI-0.60, SI-0.90, whose values are 3.03, 3.06, 3.06, 3.08 eV. It indicates that the content of anatase in TiO_2 would influence the band gap value of TiO_2. However, with the presence of anatase in the mixture as shown in Fig. 5, the light absorption of rutile is obviously lower than that of anatase/rutile mixed phase in the range between 250 and 400 nm. The lower light absorption may result in a lower photocatalytic activity, because the UV irradiation was utilized for the photocatalytic reaction.

3.2. Possible formation mechanism of TiO_2 with controlled phases

TiO_2 crystals (anatase, brookite, and rutile) consist of $[TiO_6]$ octahedra and differ only in the connection by corners or edges, and the TiO_2 formation mechanism is generally discussed on the basis of the "partial charge model" [14–16,24]. In the present work, urea acts as an effective "in situ pH adjusting reagent", which produces OH^- ions via the hydrolysis at above 85 °C and can increase pH values. $TiCl_3$ is chosen as the titanium source, and Ti^{3+} exhibits a strong tendency to form $[Ti(OH)_x(OH_2)_{6-x}]^{3-x}$ species via hydrolysis, due to its the high charge/radius ratio (the possible coordination of Cl^- is tentatively not considered) [27]. According to the "partial charge model", the linking of $[TiO_6]$ units in TiO_2 is formed by condensation of octahedral $[Ti(OH)_x(OH_2)_y]^{n+}$ precursor ions.

The initial pH of aqueous phase is very low (about 0.2 in series I), and it does not change much when the addition amount of urea is ≤0.30 g. Under this condition, the rutile formation undergoes as follows [28]:

$$[Ti(H_2O)_6]^{3+} + H_2O \rightarrow [TiOH(H_2O)_5]^{2+} + H_3O^+$$

$$[TiOH(H_2O)_5]^{2+} + O_2 \rightarrow \text{Ti(IV) oxo species} \rightarrow TiO_2$$

$[TiOH(H_2O)_5]^{2+}$ is first produced by hydrolysis of $[Ti(H_2O)_6]^{3+}$ and then can be oxidized by dissolved oxygen to form Ti(IV) oxo species. The Ti(IV) oxo species is assumed to be an intermediate between TiO^{2+} and TiO_2, consisting of partly dehydrated polymeric Ti(IV) hydroxide [29,30], and they can only occur the corner-sharing bonding, which leads to the formation of rutile phase.

With increasing the addition of urea to the reaction medium, the acidity would decrease (high pH), and the degree of hydrolysis would increase, thus leading to an increase of the number of OH coordinated to Ti centers. A general simplified scheme of process is given:

$$[Ti(H_2O)_6]^{3+} + OH^- \rightarrow [Ti(OH)_x(H_2O)_{6-x}]^{3-x}$$

$$\rightarrow [Ti(OH)_3(H_2O)_3]^0 \rightarrow [Ti(OH)_4(H_2O)_2]^0 \rightarrow TiO_2$$

At high pH values, the number of OH ligands (x) is high. If the produced OH^- is more enough by hydrolysis of urea, a zero-charge complex ($[Ti(OH)_3(H_2O)_3]^0$) will be formed, which can be oxidized to $[Ti(OH)_4(H_2O)_2]^0$ quickly. $[Ti(OH)_x(H_2O)_{6-x}]^{3-x}$ monomers can form different structures of polymers by sharing edges or corners, which lead to different phases of TiO_2. The formation of edge-shared bonding requires two oxolation reactions between pairs of Ti centers to occur simultaneously. At lower acidity, more OH ligands coordinated to Ti centers. Consequently, the probability of edge-shared bonding is increased, and it promotes the formation of the anatase phase.

The results of series II further demonstrate these viewpoints mentioned above. The acidity in aqueous phase of series II is much higher than that of series I. Therefore, the required amount of urea to control the phase in series II is much bigger than that in series I. It is showed apparently by comparing with the XRD patterns of two series.

3.3. Photocatalytic activity of mixed-phase TiO_2 products

The photocatalytic activity of the resulting samples with different contents of anatase was evaluated by analyzing the decolorization and the total organic carbon (TOC) removal rate of Rhodamine B (20 mg L^{-1}) in an aqueous solution under a 300 W UV lamp for 2 h (Fig. 6). The residual Rhodamine B in the solution was analyzed by checking the absorbance at 552 nm. As shown in Fig. 6, the photocatalytic activity of the samples depended on the anatase/rutile ratio. The photocatalytic decolorization of Rhodamine B increased significantly at the beginning, and then showed

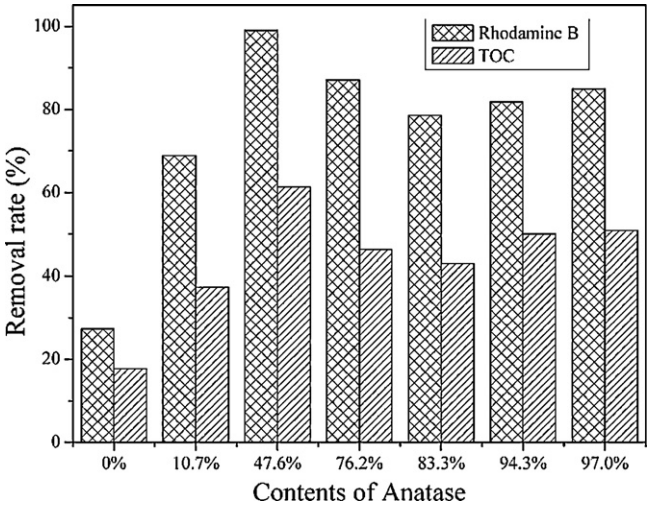

Fig. 6. Removal rate of Rhodamine B and the TOC for the photocatalytic decomposition with different TiO_2 catalysts in Series I from left to right: SI-0.30, SI-0.35, SI-0.40, SI-0.50, SI-0.60, SI-0.90, and SI-1.80.

a downtrend with increasing the anatase content. The TOC removal rate also revealed the same tendency of the photocatalytic decomposition with optimum activity at an anatase content of 47.6%, which was better than that of Degussa P25. Commercial TiO_2 Degussa P25 was also investigated for comparison, which is composed of about 80% anatase and 20% rutile. The photocatalytic activity of P25 was not illustrated in Fig. 6; the degradation of Rhodamine B under UV in 2 h was 90% and the mineralization of TOC was 55%. Among the products prepared under different amounts of urea, pure rutile obtained with addition of 0.30 g shows the lowest activity, where only 27.3% Rhodamine B was decolorized and 17.7% of TOC was mineralized. The photocatalytic degradation could be significantly increased when as-prepared samples were composed of anatase/rutile mixed phase, comparing with that of pure rutile (Fig. 6). A mixture containing 52.4% rutile and 47.6% anatase was achieved by adding 0.40 g of urea, and showed the highest photocatalytic activity, where the degradation percentage of Rhodamine B was as high as 99% and the mineralization rate of TOC was 62%. However, the photocatalytic activity of as-prepared products decreased when the anatase proportion was more than 47.6%. It is often assumed that the larger the surface area, and thus the higher the adsorption of the organic molecules, the higher will be the photocatalytic degradation rate. The BET surface areas of all samples are shown in Table 1. The S_{BET} values show the uptrend with an increase of the anatase content. The S_{BET} of SI-0.40 with the highest photocatalytic activity is only 62 m^2/g. The photocatalytic activity of samples in series I first increases with increasing surface areas, followed by a downtrend of activity with increasing S_{BET}. These results imply that BET surface area is not the main factor for photocatalytic activity in this system. Thus, these can be explained by the reason that the anatase/rutile mixed phase has a synergistic effect in enhancing the photocatalytic activity. It is the fact that the conduction band edge of anatase (E_g = 3.14) is 0.16 eV more negative than that of rutile (E_g = 2.98), and it is implied to promote interfacial electron transfer from anatase into rutile, and the energy barrier will suppress back electron transfer. Consequently, the anatase/rutile mixed phase will lead to better charge separation and thus to an increase of the photocatalytic activity. On the other hand, the anatase/rutile mixed phase could extend the useful range of the photoresponse and absorb more light, according to the narrower band gap of rutile. When the content of rutile is too much, it would inhibit the photoexcition carried in the anatase phase, resulting in a lower photocatalytic activity. It is generally suggested that the pure anatase has a higher photocatalytic activity than the rutile phase. When the content of rutile in mixed-phase TiO_2 is too little, the lower activity can be explained by geometric considerations. The rutile may be covered by too many anatase nanoparticles, and the charge separation would be limited to some extent, which leads to lower photocatalytic activity. Thus, the optimum ratio of anatase to rutile was found to be about 1:1 in this experimental system.

Comparing with series I, the photocatalytic activity of samples in series II have also been achieved, whose photodegradation of Rhodamine B are 48.2%, 74%, 73.3% and 90% in the order of SII-0.90, SII-1.20, SII-1.50 and SII-1.80. The photocatalytic activity of samples in series II increases as the content of the anatase phase in TiO_2 increases. SII-1.80 exhibits the highest activity, whose composition and photodegradation rate of Rhodamine B is similar to those of P25. The difference of photodegradation rate between series I and II may be caused by the different composition of phases, BET surface areas and morphologies of TiO_2 powders.

4. Conclusion

In summary, pure rutile and rutile–anatase mixed-phase have been successfully synthesized by a microemulsion-mediated solvothermal treatment of titanium trichloride with the assistance of urea. The contents of anatase in the products can be controlled by simply changing the amount of urea in the aqueous phase. A possible explanation of formation mechanism was proposed, based on the influence of amount of urea. The composition of the aqueous phase in microemuslion influences not only the crystalline phase but also the morphologies of final products. The as-prepared TiO_2 containing 47.6% anatase and 52.4% rutile presented the highest photocatalytic activity for decomposition of Rhodamine B, due to the existence of a synergistic effect between anatase and rutile.

Acknowledgments

This work has been supported by National Nature Science Foundation of China (20773039, 20977030), National Basic Research Program of China (973 Program, 2007CB613301, 2010CB732306), Science and Technology Commission of Shanghai Municipality (10520709900, 10JC1403900) and the Fundamental Research Funds for the Central Universities.

References

[1] M.R. Hoffmann, S.T. Martin, W. Choi, D.W. Bahnemann, Environmental applications of semiconductor photocatalysis, Chem. Rev. 95 (1995) 69–96.
[2] T.L. Thompson, J.T. Yates, Surface science studies of the photoactivation of TiO_2-new photochemical process, Chem. Rev. 106 (2006) 4428–4453.
[3] A. Fujishima, T.N. Rao, D.A. Tryk, Titanium dioxide photocatalysis, J. Photochem. Photobiol. C: Photochem. Rev. 1 (2000) 1–21.
[4] J. Zhu, W. Zheng, B. He, J. Zhang, M. Anpo, Characterization of Fe-TiO_2 photocatalysts synthesized by hydrothermal method and their photocatalytic reactivity for degradation of XRG dye diluted in water, J. Mol. Catal. A 216 (2004) 35–43.
[5] J.L. Zhang, Y. Hu, M. Matsuoka, H. Yamashita, M. Minagawa, H. Hidaka, M. Anpo, Relationship between the local structures of titanium oxide photocatalysts and their reactivities in the decomposition of NO, J. Phys. Chem. B 105 (2001) 8395–8398.
[6] G.H. Tian, H.G. Fu, L.Q. Jing, C.G. Tian, Synthesis and photocatalytic activity of stable nanocrystalline TiO_2 with high crystallinity and large surface area, J. Hazard. Mater. 161 (2009) 1122–1130.
[7] B. Zhao, F. Chen, Q.W. Huang, J.L. Zhang, Brookite TiO_2 nanoflowers, Chem. Commun. 34 (2009) 5115–5117.
[8] J.H. Zhang, X. Xiao, J.M. Nan, Hydrothermal-hydrolysis synthesis and photocatalytic properties of nano-TiO_2 with an adjustable crystalline structure, J. Hazard. Mater. 176 (2010) 617–622.
[9] M.C. Yan, F. Chen, J.L. Zhang, M. Anpo, Preparation of controllable crystalline titania and study on the photocatalytic properties, J. Phys. Chem. B 109 (2005) 8673–8678.
[10] H. Xu, L.Z. Zhang, Controllable one-spot synthesis and enhanced photocatalytic activity of mixed-phase TiO_2 nanocrystals with tunable brookite/rutile ratios, J. Phys. Chem. C 113 (2009) 1785–1790.

[11] J.P. Wei, J.F. Yao, X.Y. Zhang, W. Zhu, H. Wang, M.J. Rhodes, Hydrothermal growth of titania nanostructures with tunable phase and shape, Mater. Lett. 61 (2007) 4610–4613.
[12] J.C. Yu, L. Zhang, J.G. Yu, Direct sonochemical preparation and characterization of highly active mesoporous TiO_2 with a bicrystalline framework, Chem. Mater. 14 (2002) 4647–4653.
[13] J.C. Yu, J.G. Yu, W.K. Ho, L.Z. Zhang, Preparation of highly photocatalytic nanosized TiO_2 particles via ultrasonic irradiation, Chem. Commun. 19 (2001) 1942–1943.
[14] S.T. Aruna, S. Tirosh, A. Zaban, Nanosized rutile particle synthesis via hydrothermal method without mineralizers, J. Mater. Chem. 10 (2000) 2388–2391.
[15] Y.Q. Zheng, E.W. Shi, Z.Z. Chen, W.J. Li, X.F. Hu, Influence of solution concentration on the hydrothermal preparation of titania crystallites, J. Mater. Chem. 11 (2001) 1547–1551.
[16] S. Yin, H. Hasegawa, D. Maeda, M. Ishitsuka, T. Sato, Synthesis of visible light active nanosize rutile titania photocatalyst by low temperature dissolution–reprecipitation process, J. Photochem. Photobiol. A 163 (2004) 1–8.
[17] M.M. Wu, J.B. Long, A.H. Huang, Y.J. Luo, S.H. Feng, R.R. Xu, Microemulsion-mediated hydrothermal synthesis and characterization of nanosize rutile and anatase particles, Langmuir 15 (1999) 8822–8825.
[18] C.H. Lu, W.H. Wu, R.B. Kale, Microemuslion-mediated hydrothermal synthesis of photocatalytic TiO_2 powders, J. Hazard. Mater. 154 (2008) 649–654.
[19] H.Z. Zhang, J.F. Banfield, Understanding polymorphic phase transformation behavior during growth of nanocrystalline aggregates: insights from TiO_2, J. Phys. Chem. B 104 (2000) 3481–3487.
[20] G.A. Tompsett, G.A. Bowmaker, R.P. Cooney, J.B. Metson, K.A. Rogers, J.M. Seakins, The raman spectrum of brookite TiO_2, J. Raman Spectrosc. 26 (1995) 57–62.
[21] Y.H. Zhang, C.K. Chan, J.F. Porter, W.J. Guo, Micro-Raman spectroscopic characterization of nanosized TiO_2 powders prepared by vapor hydrolysis, J. Mater. Res. 13 (1998) 2602–2609.
[22] B.Z. Tian, F. Chen, J.L. Zhang, M. Anpo, Influences of acids and salts on the crystalline phase and morphology of TiO_2 prepared under ultrasound irradiation, J. Colloid Interface Sci. 303 (2006) 142–148.
[23] Q. Huang, L. Gao, A simple route for the synthesis of rutile TiO_2 nanorods, Chem. Lett. 32 (2003) 638–639.
[24] H. Cheng, J. Ma, Z. Zhao, L. Qi, Hydrothermal preparation of uniform nanosized rutile and anatase particles, Chem. Mater. 7 (1995) 663–671.
[25] N. Serpone, D. Lawless, R. Khairutidinov, J. Phys. Chem. 99 (1995) 16646–16654.
[26] A.L. Linsebigler, G.Q. Lu, J.T. Yates, Photocatalysis on TiO_2 surfaces: principles, mechanisms, and selected results, Chem. Rev. 95 (1995) 735–758.
[27] M. Henry, J.P. Jolivet, J. Livage, Aqueous Chemistry of Metal Cations, Hydrolysis, Condensation, and Complexation, Springer-Verlag, Berlin, 1992.
[28] E. Hosono, S. Fujihara, K. Kakiuchi, H. Imai, Growth of submicrometer-scale rectangular parallelepiped rutile TiO_2 films in aqueous $TiCl_3$ solutions under hydrothermal conditions, J. Am. Chem. Soc. 126 (2004) 7790–7791.
[29] L. Kavan, B. O'Regan, A. Kay, M. Grätzel, Preparation of TiO_2(anatase) films on electrodes by anodic oxidative hydrolysis of $TiCl_3$, J. Electroanal. Chem. 346 (1993) 291–307.
[30] F.P. Rotzinger, M. Grtäzel, Characterization of the perhydroxytitanyl(2+) ion in acidic aqueous solution. Products and kinetics of its decomposition, Inorg. Chem. 26 (1987) 3704–3708.